

COMPUTER SIMULATION OF VERTICALLY AND HORIZONTALLY PHASED CYLINDRICAL SONAR ARRAYS

J. Cibis and M.-Th. Roeckerath-Ries

Krupp Atlas Elektronik GmbH, Bremen

1. INTRODUCTION

In the development of a three-dimensional high-resolution sonar system, the design of a vertically and horizontally phased three-dimensional array is very important. This paper presents the results of the examination of beam-pattern for a vertically and horizontally phased cylindrical array. In [3] some results of a computer simulation of horizontal beam-pattern for horizontally phased cylindrical arrays are given. Here we are especially interested in the vertical pattern of vertically phased arrays. The problem of generating variable horizontal and vertical beamwidths by "spatial frequency modulation" will be dealt with as well as steering the beam in the horizontal and vertical direction. In particular, for cylindrical arrays with $H \ll R$, where H and R denote the height and radius of the cylinder, the pattern is significantly influenced by the Bessel-function induced by the curvature of the array. This phenomenon will be considered in the following.

In the first part of this paper, some theoretical derivations for the pattern of transparent phased cylindrical arrays are given. The second part outlines the results of the numerical simulation approach. Some horizontal and vertical patterns, as well as three-dimensional ones are presented.

2. THEORETICAL DERIVATION OF THE THREE-DIMENSIONAL BEAM-PATTERN OF A CYLINDRICAL ARRAY

2.1 Horizontal and Vertical Beam-Steering

In general, the pattern function $B(\mathbf{f}_r)$ of an arbitrary three-dimensional aperture function $b(\mathbf{r})$ is given by the three-dimensional Fourier transform

$$B(\mathbf{f}_r) = \int b(\mathbf{r}) e^{i2\pi \mathbf{f}_r \mathbf{r}} d\mathbf{r}, \quad (1)$$

where \mathbf{f}_r is a vector indicating the direction of arrival of a monochromatic plane wave of wavelength λ . Using azimuth and elevation angles θ_h and θ_v , the components of \mathbf{f}_r are given by

$$f_x = (\sin\theta_h \cos\theta_v)/\lambda, \quad f_y = (\cos\theta_h \cos\theta_v)/\lambda, \quad f_z = (\sin\theta_v)/\lambda. \quad (2)$$

A "translation" of the pattern function in the three-dimensional space by a "steering vector" $\mathbf{f}_{rs} = (f_{xs}, f_{ys}, f_{zs})$ is caused by phasing the aperture function

PHASED CYLINDRICAL SONAR ARRAYS

$$b(\mathbf{r}) \rightarrow b(\mathbf{r}) e^{-i2\pi \mathbf{f}_{r_s} \cdot \mathbf{r}} \quad (3)$$

The corresponding pattern function changes to

$$B_s(\mathbf{f}_r) := \int b(\mathbf{r}) e^{i2\pi(\mathbf{f}_r - \mathbf{f}_{r_s}) \cdot \mathbf{r}} d\mathbf{r} = B(\mathbf{f}_r - \mathbf{f}_{r_s}) \quad (4)$$

The aperture function of a transparent cylindrical array of height H and radius R (Fig. 1) is given by

$$b(\mathbf{r}) = \text{rect}\left(\frac{z}{H}\right) \delta(\sqrt{x^2 + y^2} - R) \quad (5)$$

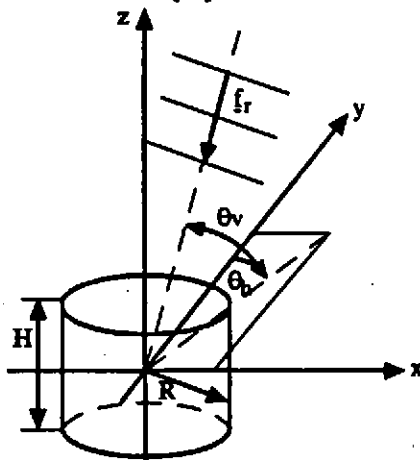


Fig. 1

and the three-dimensional Fourier transform (4) yields

$$B_s(\mathbf{f}_r) = B(\mathbf{f}_r - \mathbf{f}_{r_s}) = 2\pi R H \text{si}(\pi H(\mathbf{f}_z - \mathbf{f}_{z_s})) J_0(2\pi R \sqrt{(\mathbf{f}_x - \mathbf{f}_{x_s})^2 + (\mathbf{f}_y - \mathbf{f}_{y_s})^2}) \quad (6)$$

The si function is defined by $\text{si}(x) := \sin(x)/x$, and J_0 denotes the Bessel-function of order zero. Since $b(\mathbf{r})$ is separable into z and (x, y) , the pattern function $B_s(\mathbf{f}_r)$ is also separable into f_z and (f_x, f_y) . The si function is the pattern function of a line array of length H and describes the stave characteristic of a cylindrical array, whereas the Bessel-function gives the pattern of a circle of radius R in the x - y plane. Depending on the relationship between H and R , either the si function or the Bessel-function gives the dominant part for the pattern function of the cylinder. For $H \ll R$ in particular, this means in practice that the vertical beam-pattern cannot be approximated by the stave characteristic. For special choices of the steering vector \mathbf{f}_{r_s} the steering process results in different receiving or transmitting modes:

i) Horizontal Omnidirectional Mode (HO)

$\mathbf{f}_{r_s} = (0, 0, (\sin\theta_v)/\lambda)$ with a vertical steering angle $\theta_v \in [-\pi/2, \pi/2]$ gives a pattern function

$$B_s(\mathbf{f}_r) = 2\pi R H \text{si}(\pi H(\sin\theta_v - \sin\theta_v)/\lambda) J_0(2\pi R(\cos\theta_v)/\lambda) \quad (7)$$

PHASED CYLINDRICAL SONAR ARRAYS

This results in a horizontal omnidirectional mode with vertical steering into the direction θ_{v_s} . The pattern function does not depend on the angle θ_h of horizontal incidence. The vertical pattern depends on H as well as R . For $H \ll R$, the Bessel-function is not negligible and results in vertical side-lobes at $\theta_v = \pm \pi/2$.

ii) Horizontally Steered Mode (HS)

$\mathbf{f}_{r_s} = (\sin\theta_{h_s} \cos\theta_{v_s}, \cos\theta_{h_s} \cos\theta_{v_s}, \sin\theta_{v_s}) / \lambda$, with vertical and horizontal steering angles $\theta_{v_s} \in [-\pi/2, \pi/2]$ and $\theta_{h_s} \in [-\pi, \pi]$, respectively, gives a pattern function which depends on the vertical and horizontal angles of incidence. The horizontal and vertical patterns are produced by cuts through the three-dimensional one (7).

$\theta_h = \theta_{h_s}$ yields the vertical pattern

$$B_{s,ver}(f_r) = 2\pi RH \operatorname{si}(\pi H(\sin\theta_v - \sin\theta_{v_s})/\lambda) J_0(2\pi R(\cos\theta_v - \cos\theta_{v_s})/\lambda) \quad (8)$$

as the product of the shifted si and Bessel-function. For a very flat cylinder ($H \ll R$), the beam-pattern is dominated by the Bessel-function. This means that, in the HS mode, the vertical beamwidth is determined more by the radius than by the height of the antenna. Because the cosine term in the Bessel-function is symmetrical relative to zero, steering into the vertical direction θ_{v_s} results in a second side-lobe at $-\theta_{v_s}$, which is more or less suppressed by the si function. Steering to θ_{v_s} results in a "broadening" of the si term but a "narrowing" of the Bessel-term in (8). Combining these two effects, this means that, even if the dimensions of the cylinder are chosen such that the resulting vertical beamwidth in the unsteered case is mainly given by the stave characteristic (si function), the vertical steering can lead to substantially narrowed vertical beamwidths.

$\theta_v = \theta_{v_s}$ results in the horizontal pattern

$$B_{s,hor}(f_r) = 2\pi RH J_0(2\pi R \cos\theta_{v_s} 2 \sin((\theta_h - \theta_{h_s})/2)/\lambda) . \quad (9)$$

The HS mode can roughly be interpreted as a process in which all the transducer signals are compensated onto a plane perpendicular to the steering vector \mathbf{f}_{r_s} (see Fig. 2).

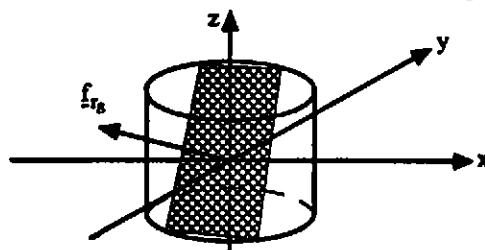


Fig. 2

PHASED CYLINDRICAL SONAR ARRAYS

Similar to broadening the spectrum of a narrowband time signal by frequency modulation (for details see [2]), the horizontal and vertical beamwidths of a pattern function can be extended by modulation of the "spatial frequency". Horizontal beam-broadening only makes sense for the HS mode, whereas vertical broadening is efficient for HO and HS mode as well, but different effects appear.

2.2 Beam-Broadening by Spatial Frequency Modulation

To describe the method of horizontal and vertical steering and broadening simultaneously, first some notations have to be defined. Let θ_{v_0} and θ_{h_0} denote the vertical and horizontal steering angles, θ_{v_b} and θ_{h_b} some adjusting angles to control the vertical and horizontal beamwidths, β the angular participating region of the aperture, and $\varphi(r)$ the angular coordinate of r in the x-y plane (Fig. 3). Because in practice the cylindrical array is not transparent, in the HS mode only an angular aperture $\beta \ll 180^\circ$ is activated.

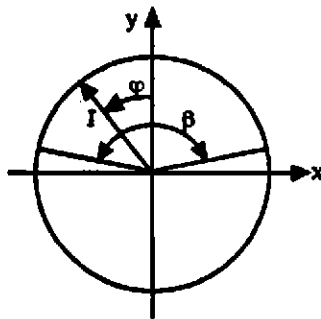


Fig. 3

For each position r define the "steering angles"

$$\theta_{v_s}(r) = \theta_{v_b} z/H + \theta_{v_0} \quad \text{and} \quad \theta_{h_s}(r) = \theta_{h_b} \varphi(r)/\beta + \theta_{h_0}. \quad (10)$$

By (10) the "spatial three-dimensional frequency modulation" is described, and for each position r a "steering vector" $f_{r_s}(r)$ is given by

$$f_{r_s}(r) = (\sin\theta_{h_s}(r) \cos\theta_{v_s}(r), \cos\theta_{h_s}(r) \cos\theta_{v_s}(r), \sin\theta_{v_s}(r)) / \lambda. \quad (11)$$

By the phasing $b(r) \rightarrow b(r) e^{-i2\pi f_{r_s}(r) \cdot r}$ the desired steering of the pattern to $(\theta_{h_0}, \theta_{v_0})$ and the simultaneous broadening of the horizontal and vertical beamwidths are achieved. As already mentioned, horizontal beam-steering as well as horizontal beam-broadening during HO mode does not make any sense. In this omnidirectional mode, choose

$$f_{r_s}(r) = (0, 0, \sin\theta_{v_s}(r)) / \lambda. \quad (12)$$

PHASED CYLINDRICAL SONAR ARRAYS

By (12) the procedure is reduced to a purely vertical process.

Beam-broadening by phase shading produces a ripple in the pattern, which can be effectively reduced by filtering. For this purpose it is sufficient to use a taper which only flattens the steep flanks at the ends of the aperture function.

3. COMPUTER SIMULATION APPROACH

For the simulation process, the aperture function $b(r)$ is spatially sampled. The horizontal as well as the vertical element spacing on the antenna is chosen as $d = \lambda/2$ and the normalized three-dimensional pattern $B_T(f_r)$ of the single transducer element is assumed to be

$$B_T(f_r) = \text{si}(\pi d f_r) \text{si}(\pi d f_r) . \quad (13)$$

In addition to the characteristics of the elements themselves, it is taken into consideration that, in contrast to our theoretical calculations, the array is not transparent. For further details, see [1]. This reduces the theoretically derived effects of the Bessel-function. The beam-patterns given as $20\log|B(f_r)|$ are normalized to 0 dB and have been calculated for HO and HS mode with and without beam-broadening and filtering.

Figs. 4-6 show the described effects of flat cylindrical arrays in HO and HS mode. Fig. 4 demonstrates the side-lobes at $\theta_v = \pm \pi/2$ in the vertical pattern for HO mode. Fig. 5 shows the effect of limiting the vertical beamwidth by the Bessel-function in HS mode. Additionally, the stave characteristic is given. In Fig. 6 the narrowing of the vertically steered beam, as well as the symmetrical side-lobe at $-\theta_v$, in the vertical pattern for HS mode can be seen.

The described method (11) gives very good results for both directions, especially for a planar array of length L and height H . In this case, the angular aperture β and the angular coordinate $\varphi(r)$ in (10) have to be replaced by the length L and the x -coordinate of the position r , respectively. Fig. 7 and 8 demonstrate horizontal and vertical beam-broadening for a planar array. For a cylindrical array, horizontal steering and beamforming in HS mode are mainly reduced by the transducer pattern function and the "shadowing" of the array. Fig. 9 shows the horizontal pattern with and without horizontal broadening for the unsteered case. In Fig. 10 the reduction of the ripple by filtering can be seen. In Fig. 11 the beam is additionally horizontally steered.

Vertical beam-broadening and steering at the same time leads to satisfactory results for a cylinder with $H = R$. Fig. 12 gives the vertically broadened and unbroadened pattern of a cylinder with

PHASED CYLINDRICAL SONAR ARRAYS

$H = 2R$. In Fig. 13 the broadened vertical pattern is additionally steered. For $H \ll R$ the procedure of simultaneous vertical broadening and steering would have failed. Already, vertical steering without broadening yields narrowed beams deformed by the Bessel-function. This means that, with this phasing method, it is not possible to produce "arbitrary" wide vertical beamwidths.

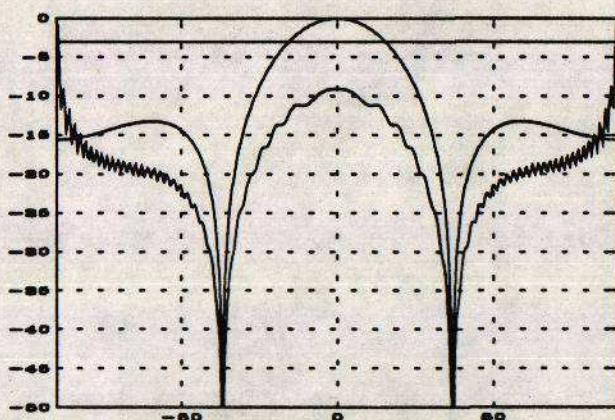


Fig. 4 Vertical pattern of a cylindrical array in HO mode
 $f=100\text{kHz}$; $R=50\text{cm}$; $H=2,5\text{cm}$;
 $\theta_{hs}=0^\circ$; $\theta_{vs}=0^\circ$; $\theta_{hb}=0^\circ$; $\theta_{vb}=0^\circ$;

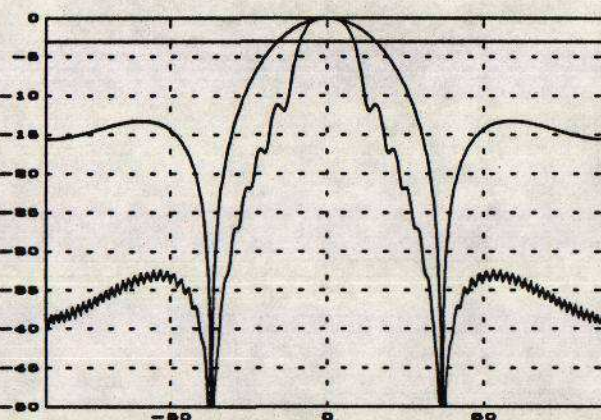


Fig. 5 Vertical pattern of a cylindrical array in HS mode
 $f=100\text{kHz}$; $R=50\text{cm}$; $H=2,5\text{cm}$;
 $\theta_{hs}=0^\circ$; $\theta_{vs}=0^\circ$; $\theta_{hb}=0^\circ$; $\theta_{vb}=0^\circ$;

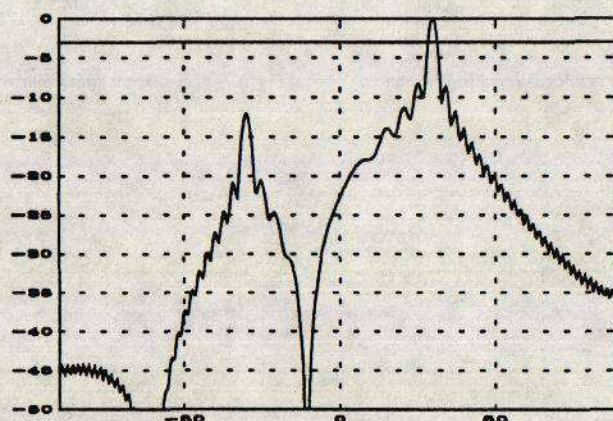


Fig. 6 Vertical pattern of a cylindrical array in HS mode
 $f=100\text{kHz}$; $R=50\text{cm}$; $H=2,5\text{cm}$;
 $\theta_{hs}=0^\circ$; $\theta_{vs}=30^\circ$; $\theta_{hb}=0^\circ$; $\theta_{vb}=0^\circ$;

PHASED CYLINDRICAL SONAR ARRAYS

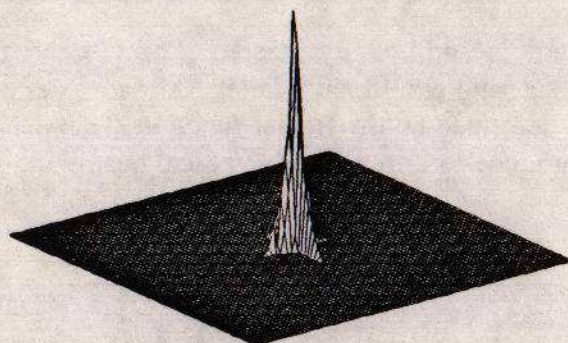


Fig. 7 Pattern of a planar array
 $f=100\text{kHz}$; $L=50\text{cm}$; $H=40\text{cm}$;
 $\theta_{h_s}=0^\circ$; $\theta_{v_s}=0^\circ$; $\theta_{h_b}=0^\circ$; $\theta_{v_b}=0^\circ$;

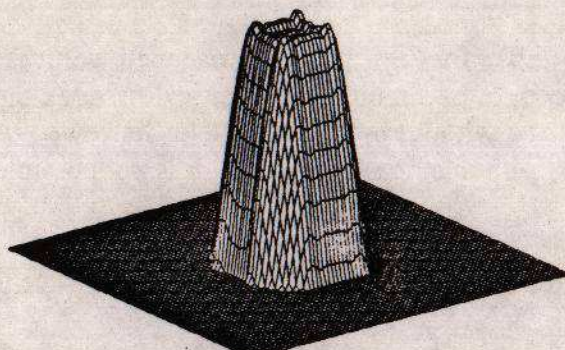


Fig. 8 Pattern of a planar array
 $f=100\text{kHz}$; $L=50\text{cm}$; $H=40\text{cm}$;
 $\theta_{h_s}=0^\circ$; $\theta_{v_s}=0^\circ$; $\theta_{h_b}=20^\circ$; $\theta_{v_b}=20^\circ$;

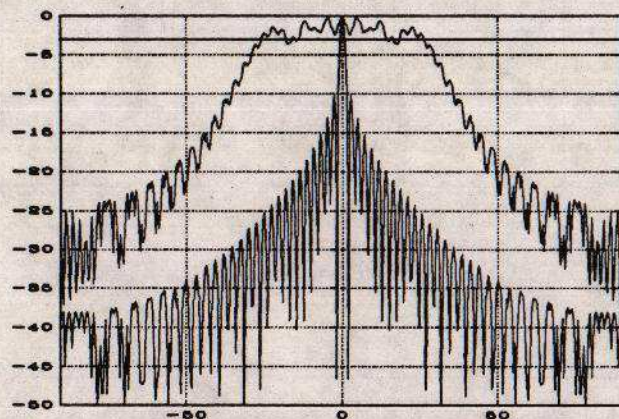


Fig. 9 Horizontal pattern of a cylindrical array in HS mode
 $f=100\text{kHz}$; $R=20\text{cm}$; $H=2.5\text{cm}$;
 $\theta_{h_s}=0^\circ$; $\theta_{v_s}=0^\circ$; $\theta_{h_b}=30^\circ$; $\theta_{v_b}=0^\circ$;

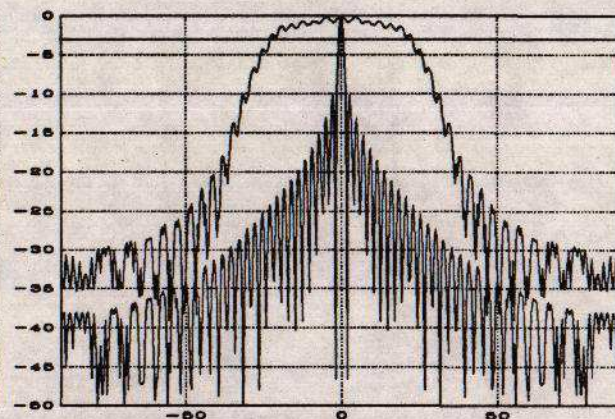


Fig. 10 Horizontal pattern of a cylindrical array in HS mode
 $f=100\text{kHz}$; $R=20\text{cm}$; $H=2.5\text{cm}$;
 $\theta_{h_s}=0^\circ$; $\theta_{v_s}=0^\circ$; $\theta_{h_b}=30^\circ$; $\theta_{v_b}=0^\circ$;

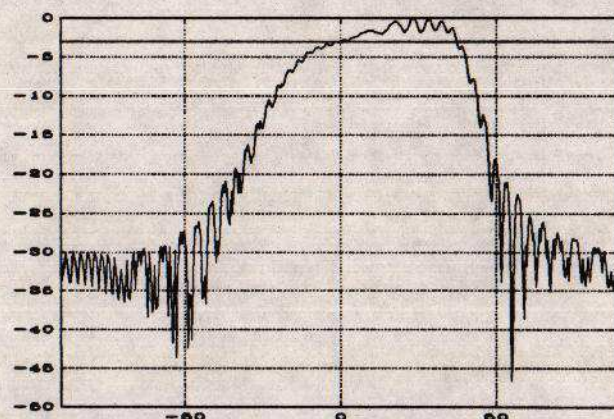


Fig. 11 Horizontal pattern of a cylindrical array in HS mode
 $f=100\text{kHz}$; $R=20\text{cm}$; $H=2.5\text{cm}$;
 $\theta_{h_s}=20^\circ$; $\theta_{v_s}=0^\circ$; $\theta_{h_b}=30^\circ$; $\theta_{v_b}=0^\circ$;

PHASED CYLINDRICAL SONAR ARRAYS

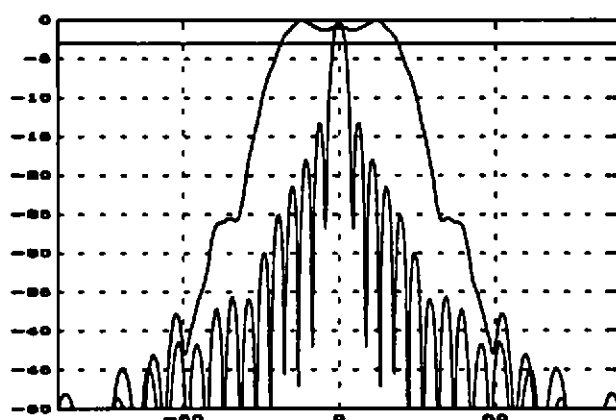


Fig. 12 Vertical pattern of a cylindrical array in HS mode
 $f=100\text{kHz}$; $R=10\text{cm}$; $H=20\text{cm}$;
 $\theta_{hs}=0^\circ$; $\theta_{vs}=0^\circ$; $\theta_{hb}=0^\circ$; $\theta_{vb}=30^\circ$;

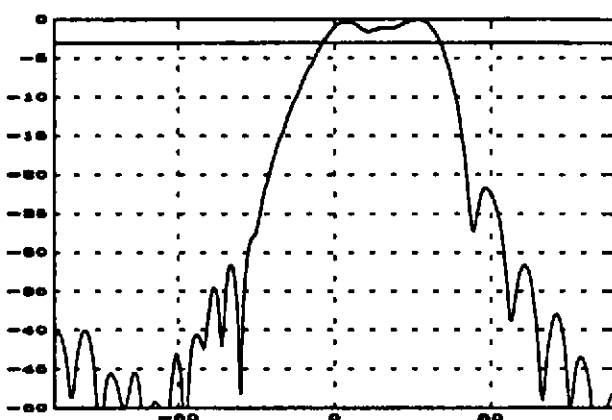


Fig. 13 Vertical pattern of a cylindrical array in HS mode
 $f=100\text{kHz}$; $R=10\text{cm}$; $H=20\text{cm}$;
 $\theta_{hs}=0^\circ$; $\theta_{vs}=20^\circ$; $\theta_{hb}=0^\circ$; $\theta_{vb}=30^\circ$;

4. CONCLUSIONS

The main result of the examination of cylindrical arrays is that the design of flat arrays ($H \ll R$) in particular, has to be treated very carefully. In this case, the vertical beam-pattern differs considerably from the stave characteristic. It can be said that it is not in general possible to generate arbitrary combinations of horizontal and vertical beamwidths. If $H \approx R$ these effects can be neglected.

5. REFERENCES

- [1] J. CIBIS and M.TH. ROECKERATH-RIES, 'Simulationsprogramm zur Berechnung dreidimensionaler Richtcharakteristiken von Zylinder- und Planarantennen bei deterministischer oder zufälliger Wandleranordnung', Krupp Atlas Elektronik GmbH, Bremen, BL 4788T102, 1991
- [2] A. PAPOULIS, 'Signal Analysis', McGraw-Hill, 1984
- [3] A. STEPNOWSKI, J. SZCZUCKA and L. PANKIEWICZ, 'Computer Simulation of Beampattern for a Sonar Phased Cylindrical Array', Progress in Underwater Acoustics, Plenum Press, New York, 1987